Chemistry & Biology, Vol. 12, 923–929, August, 2005, ©2005 Elsevier Ltd All rights reserved. DOI 10.1016/j.chembiol.2005.06.009

Calcium Ions Effectively Enhance the Effect of Antisense Peptide Nucleic Acids Conjugated to Cationic Tat and Oligoarginine Peptides

Takehiko Shiraishi, Stanislava Pankratova, and Peter E. Nielsen*
Department of Medical Biochemistry and Genetics
The Panum Institute
University of Copenhagen
Blegdamsvej 3c
2200 Copenhagen N.
Denmark

Summary

Cell-penetrating peptides have been widely used to improve cellular delivery of a variety of proteins and antisense agents. However, recent studies indicate that such cationic peptides are predominantly entering cells via an endosomal pathway. We now show that the nuclear antisense effect in HeLa cells of a variety of peptide nucleic acid (PNA) peptide conjugates is significantly enhanced by addition of 6 mM Ca^{2+} (as well as by the lysosomotrophic agent chloroquine). In particular, the antisense activities of Tat(48-60) and heptaarginine-conjugated PNAs were increased 44-fold and 8.5-fold, respectively. Evidence is presented that the mechanism involves endosomal release. The present results show that Ca^{2+} can be used as an effective enhancer for in vitro cellular delivery of cationic peptide-conjugated PNA oligomers, and also emphasize the significance of the endosomal escape route for such peptides.

Introduction

Peptide nucleic acids (PNA) have long been considered as promising candidates for the discovery and development of gene therapeutic antisense agents, but quick progress is hampered by suboptimal techniques for cellular delivery [1, 2]. Several methods are available for delivery of PNA oligomers to cells in culture. The techniques include delivery of PNA/DNA heteroduplexes [3], fatty acid- [4] or 9-aminoacridine-conjugated PNA via cationic liposomes [5, 6], and direct delivery of PNAs conjugated to a variety of cell-penetrating peptides [7, 8] or to triphenylphosphonium ligands [9]. Especially, the cell-penetrating peptide conjugates appear to offer an uncomplicated method for experiments in cell cultures. Indeed, a number of studies have reported convincing antisense activity of PNA and morpholino oligomers conjugated to such peptides [10–13], although rather high (micromolar) concentrations were required to achieve the cellular antisense effects. Furthermore, several studies have demonstrated that delivery using cationic peptides occur via the endosomal/lysosomal compartment of the cell [7, 10], thereby providing an explanation for the relatively poor antisense activity of such conjugates despite apparently effective cellular uptake when analyzed by fluorescence microscopy. Therefore, improved methods and/or protocols for cellular delivery of PNA (and other [antisense] agents) are very much warranted. In the search for such improved methods, we have synthesized a series of PNA-cationic peptide conjugates and evaluated their efficiency in an antisense assay.

We employed a sensitive luciferase-based method using HeLa pLuc705 cells [14]. The antisense molecule—targeting an aberrant splice site within intron 2—can correct mis-splicing and ensure translation of a functional luciferase protein. Therefore this splicing correction assay provides a positive readout (of luciferase activity), effectively avoiding false-positive readouts due to cellular toxicity. Furthermore, the assay reflects the number of antisense molecules delivered into the nucleus, where the antisense molecule binds to the target pre-mRNA to redirect splicing.

Endosomal escape of the antisense agent is most likely one of the major rate-limiting steps during cellular delivery via cationic peptides [7, 8, 10, 15], as it is also for delivery of DNA/polycation complexes. Recently, Zaitsev et al. [16] showed that transfection of DNA complexed with histone H1 protein is arrested in endosomes/lysosomes, and they demonstrated that addition of Ca^{2+} can enhance transfection efficiency, presumably by facilitating endosomal release. They also showed that addition of 4–6 mM of Ca^{2+} enhances the transfection of several other polycation/DNA complexes, such as HMG1/DNA, polylysine/DNA, and cationic lipid/DNA [17, 18]. Although the mechanism of the Ca^{2+} effect on transfection is not yet fully understood [16], these results prompted us to test the effect of Ca^{2+} on the antisense potency of cationic peptide-conjugated PNAs.

In this study, we demonstrate that addition of Ca^{2+} to the medium dramatically increases the nuclear antisense effect of PNA-peptide conjugates [up to 50-fold using Tat(48-60) peptide] in HeLa pLuc705 cells in culture.

Results and Discussion

In order to evaluate the effect (if any) of Ca^{2+} on the cellular delivery of PNA-peptide conjugates, a series of PNA conjugates with a range of cell-penetrating cationic peptides were synthesized and tested in the pLuc705 HeLa cell luciferase system (the nomenclature and the sequences of PNAs are listed in Table 1). In a preliminary screening, the pLuc705 HeLa cells were treated with 1 μM PNAs with or without addition of 6 mM Ca^{2+} for 24 hr and subjected to the luciferase assay (Figure 1A). Treatment with naked PNA resulted in only a 1.7-fold increase in relative light units (RLUs) relative to the control (no PNA treatment). Treatment with $(Arg)_7$-PNA or $(Arg)_9$-PNA resulted in significantly higher luciferase activity (RLUs) than the control (14-fold and 27-fold, respectively), whereas treatment with $(Arg)_6$-PNA produced only a 2.5-fold increase of RLU (which is not significantly different from naked PNA), and the remaining cationic peptide-conjugated PNAs (NLS-PNA, $[KFF]_3$-PNA, and Tat-PNA) did not show activity much higher than that of naked PNA.

*Correspondence: pen@imbg.ku.dk

Table 1. Nomenclature and Sequences of PNA-Peptide Conjugates

Names	Sequence[a]
Naked PNA	H-CCT CTT ACC TCA GTT ACA-NH2
$(Arg)_6$-PNA	H-RRRRRR-Gly-CCT CTT ACC TCA GTT ACA-NH2
$(Arg)_7$-PNA	H-RRRRRRR-Gly-CCT CTT ACC TCA GTT ACA-NH2
$(Arg)_9$-PNA	H-RRRRRRRRR-Gly-CCT CTT ACC TCA GTT ACA-NH2
$(KFF)_3$-PNA	H-KFFKFFKFFK-eg1-CCT CTT ACC TCA GTT ACA-NH2
NLS-PNA	H-PKKKRKV-eg1-CCT CTT ACC TCA GTT ACA- NH2
Tat-PNA	H-GRKKRRQRRRPPQ-eg1-CCT CTT ACC TCA GTT ACA-NH2
$(Arg)_6$-PNA-MM[b]	H-RRRRRR-Gly-CCT CT**G** ACC TCA **T**TT ACA-NH2
$(Arg)_9$-PNA-MM[b]	H-RRRRRRRRR-Gly-CCT CT**G** ACC TCA **T**TT ACA-NH2
Tat-PNA-MM[b]	H-GRKKRRQRRRPPQ-CCT CT**G** ACC TCA **T**TT ACA-NH2
$(Arg)_7$-Fl-PNA[c]	H-RRRRRRR-Fl-eg1-CCT CTT ACC TCA GTT ACA-NH2

[a] The sequences of cell-penetrating peptides are written using the standard one-letter amino acid symbols. The sequences of peptides and PNAs are written from N-terminal- to C-terminal-end.
[b] PNA-MM indicates a mismatch PNA sequence, whereas two mismatches are indicated in bold.
[c] $(Arg)_7$-Fl-PNA had fluorescein (Fl) attached to the ϵ-amino group of a lysine residue (20).

According to Haberland et al. [17], addition of Ca^{2+} (4–6 mM) can improve the efficacy of polycation (such as lysine rich nuclear proteins or polylysine)-mediated DNA transfections. Therefore, we initially tested the effect of addition of 6 mM Ca^{2+} on the antisense activity of cationic PNA-peptide conjugates. The activity of all of the PNAs, in particular that of $(Arg)_7$-PNA, $(Arg)_9$-PNA, and Tat-PNA, was increased in the presence of Ca^{2+} (5-fold, 2-fold, and 25-fold, respectively, while Ca^{2+} addition alone did not significantly induce luciferase activity). These results clearly demonstrate that Ca^{2+} dramatically enhances the antisense effect of PNAs conjugated to cationic peptides and that the magnitude of this effect differs significantly between the various peptides.

To further characterize the antisense effects of oligoarginine-conjugated PNAs, we studied these PNAs, as well as two corresponding control mismatch PNAs, more thoroughly in terms of luciferase antisense activation and cellular toxicity (Figure 1B). Without Ca^{2+} addition, treatment with naked PNA or with $(Arg)_6$-PNA at 1 μM or 2 μM resulted in no significant luciferase activation compared to the control. In contrast, treatment with $(Arg)_7$-PNA or $(Arg)_9$-PNA produced a dose-dependent increase of RLUs (13-fold and 29-fold, respectively, at 2 μM), whereas the two control mismatch PNAs, conjugated to hexaarginine or nonaarginine, were practically inactive in the assay. This polyarginine length dependency in uptake properties corroborate the result of previous reports [13, 21]. However, treatment with $(Arg)_9$-PNA decreased cellular viability to 67% at 2 μM even without Ca^{2+} addition. This toxic effect most likely originates from the 9-mer L-arginine moiety, because the mismatch PNA conjugated to nonaarginine exhibited similar toxicity. However, in the presence of Ca^{2+}, $(Arg)_7$-PNA at 2 μM was slightly more active than $(Arg)_9$-PNA without severely affecting cell viability (113-fold and 109-fold, respectively, compared with the control). These results prompted us to study further the activity of the $(Arg)_7$-PNA in combination with Ca^{2+}.

In order to optimize the Ca^{2+} concentration, $(Arg)_7$-PNA was delivered to the cells in the presence of various concentrations of Ca^{2+} (Figure 2). The $(Arg)_7$-PNA exhibited the highest activity at 6 mM Ca^{2+}. Furthermore, addition of Ca^{2+} up to 6 mM did not result in severe cellular toxicity, neither in the presence or in the absence of the PNA. However, addition of Ca^{2+} greater than 6 mM lowered the cellular viability (as well as RLU). Therefore, 6 mM Ca^{2+} appeared optimal and was used for further experiments.

Next, we compared naked PNA, $(Arg)_7$-PNA, and Tat-PNA in the presence and absence of 6 mM Ca^{2+} addition at various PNA concentrations (0.5–4.0 μM) (Figure 3A). Ca^{2+} addition resulted in higher RLU at every PNA concentration. However, the effect of Ca^{2+} is much more pronounced for $(Arg)_7$-PNA and, especially, Tat-PNA than for the naked PNA. In fact, the Tat-PNA and the $(Arg)_7$-PNA exhibited almost equal activity in the presence of Ca^{2+} despite the extremely low activity of the Tat-PNA without Ca^{2+} addition. The Tat peptide has been shown to be taken up predominantly via an endocytotic pathway [8] through the electrostatic interaction between the polycationic peptide and negatively charged cellular surface components. Thus, the dramatic effect of Ca^{2+} on Tat-PNA, but not on naked PNA, might suggest that Ca^{2+} has an effect on a process after cellular uptake, such as endosomal escape.

Increased luciferase activity (measured in RLUs) should directly reflect an increased level of corrected luciferase mRNA (produced by an antisense effect of PNA for mis-splicing correction). RT-PCR analysis was performed to obtain a semiquantitative measure of the level of correctly spliced luciferase mRNA (Figure 3B). Without Ca^{2+} addition, treatment with the $(Arg)_7$-PNA did not result in any detectable accumulation of the corrected form (142 bp) up to 2 μM (Figure 3Ba), and only 7% correction was seen at 4 μM. However, Ca^{2+} addition dramatically increased the level of corrected mRNA at every PNA concentration tested, reaching 86% at 4 μM $(Arg)_7$-PNA. In addition, we tested Tat-PNA and its mismatch (Tat-PNA-MM) (Figure 3Bb), for which the levels of the splicing corrected form were only 2% and 1% for Tat-PNA and Tat-PNA-MM, respectively, without Ca^{2+} addition. Addition of Ca^{2+} increased the corrected form to 92% at 2 μM Tat-PNA, whereas only 2% correction was detected at 2 μM Tat-PNA-MM. This Ca^{2+}-dependent increase of the corrected form by

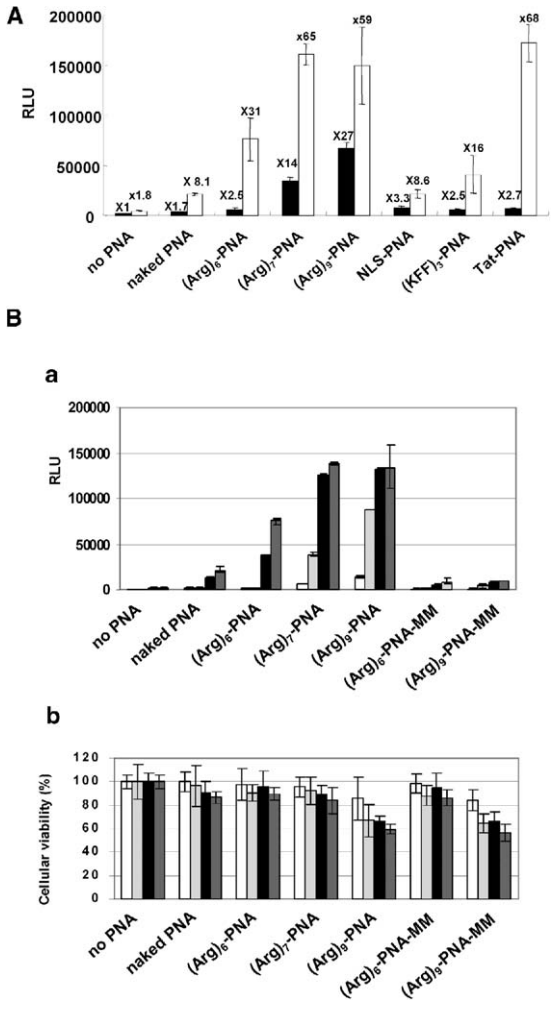

Figure 1. Effect of Ca^{2+} on the Activity of PNA-Peptide Conjugates with Different Cationic Peptides

HeLa pLc705 cells were treated with PNsA for 24 hr in the absence or presence of 6 mM Ca^{2+}. Luciferase activity was measured using Bright-Glo reagent (Promega) and is presented as relative light units (RLUs). Each bar represents the mean ± SD of three independent experiments.

(A) HeLa pLc705 cells were treated with PNAs (1 μM) for 24 hr in the absence (filled bars) or in the presence of 6 mM Ca^{2+} (white bars). The numbers on the bars indicate the fold increase of each RLU value relative to the control (no PNA, no Ca^{2+}).

(B) Effect of the numbers of arginines on the activity of polyarginine-conjugated PNAs. Polyarginine-conjugated PNA with different numbers of arginines (number of arginines; six, seven, and nine) were used. For $(Arg)_6$-PNA and $(Arg)_9$-PNA, PNAs containing two base mismatches (shown as PNA-MM) were also used as a control. White bars, PNA at 1 μM without Ca^{2+}; cross-hatched bars, PNA at 2 μM without Ca^{2+}; black bars, PNA at 1 μM with 6 mM Ca^{2+}; hatched bars, PNA at 2 μM with 6 mM Ca^{2+}. Presented are (Ba) luciferase activity and (Bb) cellular viability (expressed as relative cellular viability; the absorbance from non-PNA treated cells was set as 100%).

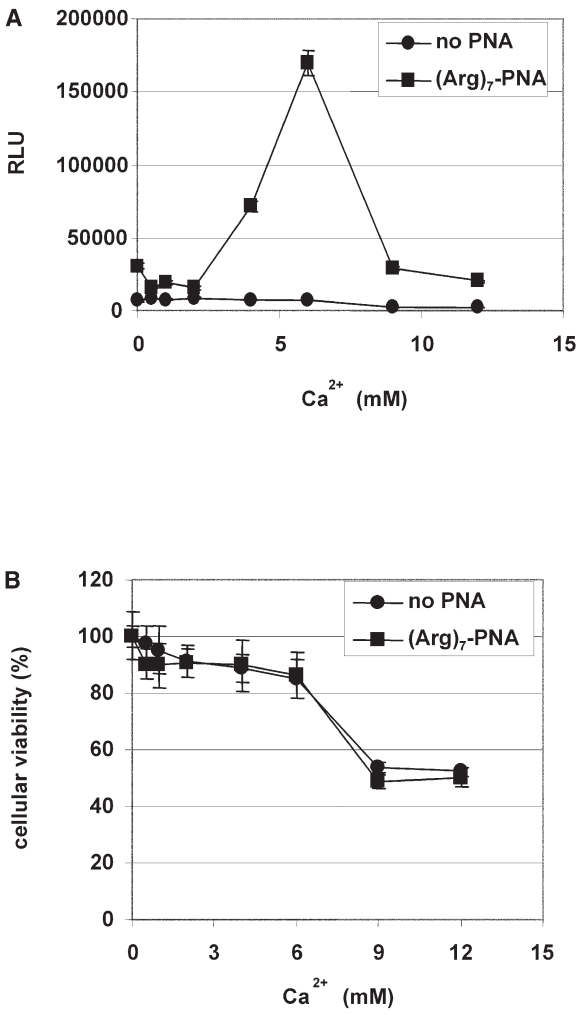

Figure 2. Effect of Ca^{2+} Concentration on the Activity of (Arg_7)-PNA

HeLa pLuc705 cells were treated with $(Arg)_7$-PNA (1 μM) for 24 hr in the presence of different concentrations of Ca^{2+}. Each data point represents the mean ± SD from three independent experiments.

(A) Luciferase activity shown as RLUs.

(B) Cellular viability (the absorbance from non-PNA treated cells without Ca^{2+} addition was set as 100%).

PNAs fully agrees with the results of the luciferase activity assay.

Uptake of $(Arg)_7$-PNA was confirmed by confocal laser scanning microscopy using fluorescein-labeled PNA ($[Arg]_7$-Fl-PNA). The pLuc-HeLa cells were treated with $(Arg)_7$-Fl-PNA (green fluorescence) for 15 min with or without Ca^{2+}, washed thoroughly, then chased in the OPTI-MEM medium for 45 min. The endocytosis marker transferrin (red fluorescence) was cotransfected with PNA. Colocalization of green and red fluorescence on the merged images (Figure 4Ac and 4Af) are seen as yellow spots. Thus, the marked colocalization of PNA with transferrin provides compelling evidence that the PNA predominantly accumulates in the endosomes, both in the absence as well as in the presence of Ca^{2+} (Figure 4A). The uptake of $(Arg)_7$-Fl-PNA occurs relatively quickly, as 15 min of incubation with PNA is sufficient for the detection of the discernible green spots in the cytoplasm (Figure 4Aa) of virtually all cells. This observation agrees with the results of the polyarginine peptide transfection studies performed by Thoren et al. [8].

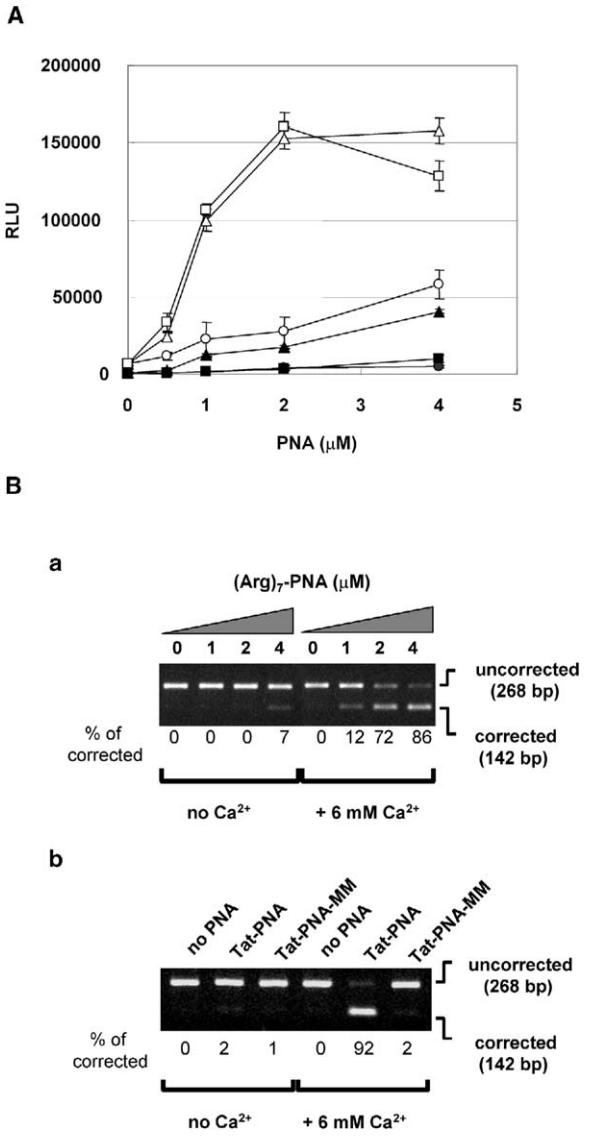

Figure 3. Effect of a 6 mM Concentration Ca^{2+} on the Activity of PNAs

HeLa pLuc705 cells were treated with PNAs at the indicated concentrations for 24 hr in the absence or presence of 6 mM Ca^{2+} and subjected to further analysis.

(A) Naked PNA (filled circle, open circle), $(Arg)_7$-PNA (filled triangle, open triangle), or Tat-PNA (filled square, open square) were used at the indicated concentrations for 24 hr in the absence (filled symbols) or presence of 6 mM Ca^{2+} (open symbols). Luciferase activity was measured using Bright-Glo reagent (Promega) and is presented as RLUs. Each data point represents the mean ± SD from three independent experiments.

(B) RT-PCR analysis of the mis-splicing correction of pre-mRNAs by PNAs. After transfection of the PNAs, total RNA was extracted and subjected to RT-PCR analysis. Uncorrected (268 bp) indicates the fragments without mis-splicing correction, and corrected (142 bp) indicates the mis-splicing corrected mRNA form. Numbers under each lane indicate the relative amount of the corrected form to the sum of corrected form and uncorrected form. (Ba) Cells were treated with $(Arg)_7$-PNAs at the indicated concentrations in the absence or presence of 6 mM Ca^{2+}. (Bb) Cells were treated with Tat-PNA (2 μM) or Tat-PNA-MM (2 μM) in the absence or presence of 6 mM Ca^{2+}. Tat-PNA-MM is a mismatch PNA containing two mismatches.

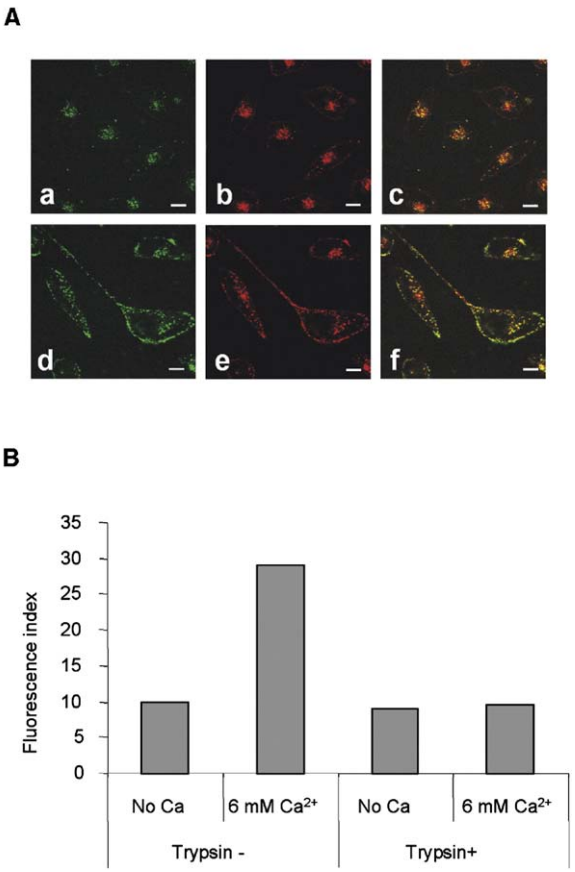

Figure 4. The Effect of 6 mM Ca^{2+} on $(Arg)_7$-Fl-PNA Cellular Uptake and Intracellular Distribution

(A) Confocal microscopic studies of $(Arg)_7$-Fl-PNA delivery to HeLa pLuc705 cells. Cells were treated with 1 μM of the PNA and 20 μg/ml transferrin for 15 min with (Ad–Af) and without (Aa–Ac) 6 mM Ca^{2+}. Cells were then washed and incubated further in OPTI-MEM medium for 45 min, and analyzed by confocal microscopy. PNA (green [Aa and Ad]), transferrin (red [Ab and Ae]) and merged images ([Ac] and [Af], respectively for [Aa and Ab] and [Ad and Ae]) are shown. Scale bars represent 35 μm.

(B) Flow cytometric analysis of the $(Arg)_7$-Fl-PNA delivery to HeLa pLuc705 cells. Cells were treated with 1 μM of PNA for 4 hr in the presence or absence of 6 mM Ca^{2+}, and harvested by scraping (trypsin–) or by trypsination (trypsin+). Cells (2000 events) were analyzed using a BD FACSCalibur cytometer, and the fluorescence index was determined by dividing the mean fluorescence of the PNA-treated sample by the mean fluorescence of a non-PNA treated sample.

Clear differences in the intracellular localization of PNA in the absence or presence of Ca^{2+} are apparent. In the absence of Ca^{2+}, PNA is seen in vesicles in the cytoplasm and in the vicinity of the nuclei (Figure 4Aa), whereas Ca^{2+} addition significantly increases the amount of complexes at the plasma membrane borders (see Figure 4Ad). However, in neither case was distinct nuclear staining observed.

Flow cytometric analysis was performed in an attempt to quantify the Ca^{2+} effect on PNA cellular delivery (Figure 4B). By collecting cells using the scraping method (Trypsin–), the fluorescence index increased

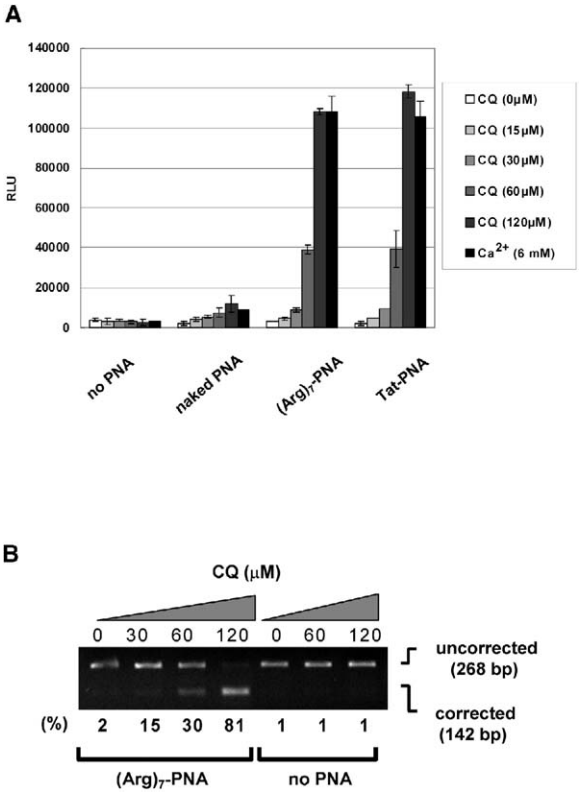

Figure 5. Effect of the Chloroquine and 6 mM Ca^{2+} on the Activity of PNA

(A) HeLa pLuc705 cells were treated with PNA in the presence of chloroquine (CQ) (15, 30, 60, and 120 μM) or Ca^{2+} (6 mM) for 24 hr. Naked PNA, $(Arg)_7$-PNA, and Tat-PNA were used at 1 μM. Luciferase activity is shown as RLUs. Each bar represents the mean ± SD from three independent experiments.

(B) RT-PCR analysis of the mis-splicing correction of pre-mRNAs by $(Arg)_7$-PNA in combination with CQ. $(Arg)_7$-PNA (1 μM) was delivered to the cells in the presence of CQ at the indicated concentrations. After 24 hr PNA incubation, the cells were subjected to RNA extraction and RT-PCR analysis as described in Figure 3B. Analogous RT-PCR results were obtained with the Tat-PNA.

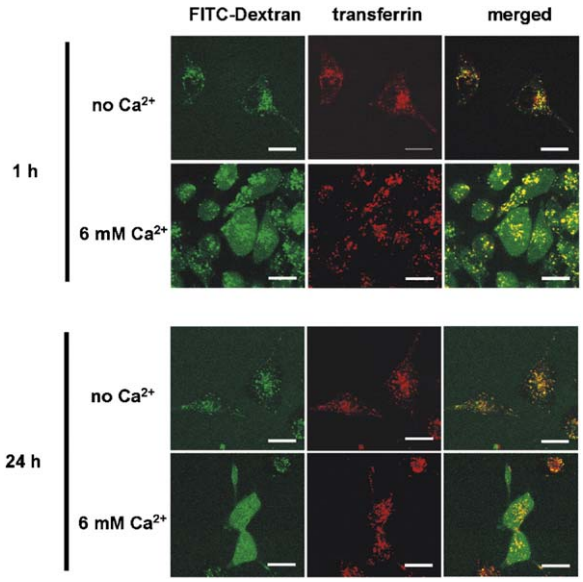

Figure 6. Effect of Ca^{2+} Ions on the Intracellular Distribution of Fluid-Phase Marker Dextran

Cells were transfected with FITC-labeled dextran (10 kDa, 2 mg/ml) and Alexa Fluor 633-conjugated human transferrin (20 μg/ml) for 4 hr in the absence or presence of 6 mM Ca^{2+} and subjected to confocal microscopic studies after 1 hr or 24 hr incubation in fresh growth medium. Left, green fluorescent images from FITC-dextran; center, red fluorescence images from the Alexa Fluor 633-conjugated dextran; right, superimposed images of green and red fluorescent images. Each scale bar indicates 63 μm.

3-fold upon Ca^{2+} treatment. However, the effect of Ca^{2+} could not be detected when the cells were colleted by trypsinization (Trypsin+). These results indicate that Ca^{2+} treatment increases the interaction between the PNA and the cellular membrane (as also indicated by the confocal microscopy data), which may in turn increase (endosome-mediated) PNA internalization.

In order to further elucidate the mechanism of the Ca^{2+} effect on PNA-peptide conjugate activity, we tested the well-known lysosomotropic agent, chloroquine (CQ), which is known to facilitate release of macromolecules from endosomes [22] (Figure 5). CQ (15, 30, 60, and 120 μM) was added together with the PNAs (naked PNA, $[Arg]_7$-PNA and Tat-PNA), and the obtained RLUs were compared with those associated with Ca^{2+} addition. Addition of CQ showed a clear dose-dependent increase in RLUs for both $(Arg)_7$-PNA and Tat-PNA, but not for naked PNA. Addition of 120 μM CQ and 6 mM Ca^{2+} showed similar enhancement of the RLUs for both $(Arg)_7$-PNA and Tat-PNA without any significant cellular toxicity (data not shown), and the finding was corroborated by RT-PCR data directly showing mRNA splice correction (Figure 5B). Furthermore, CQ alone did not show significant effects on RLUs without PNA addition. These results strongly indicate that endosomal release of the PNA conjugates can be induced by lysosomotrophic agents, and at least part of the effect of Ca^{2+} may be due to a similar mechanism.

The effect of Ca^{2+} on endosomal escape was further elucidated by using dextran (10 kDa) as a fluid-phase marker (Figure 6). Cells were cotransfected with FITC-labeled dextran and Alexa Fluor-labeled transferrin in the absence or presence of 6 mM Ca^{2+} for 4 hr, and then subjected to confocal microscopic studies after further incubation (1 and 24 hr). Because we observed that most of the green fluorescence from FITC-dextran colocalized with the red fluorescence from the endocytotic marker transferrin (shown as yellow spots in the merged picture) in the absence of Ca^{2+} treatment, we conclude that most of the dextran was localized in the endosomal compartment. In contrast, FITC-dextran was localized both in the cytoplasm and endosome in the Ca^{2+}-treated cells after 1 hr incubation. Notably, no significant release of transferrin was observed in these experiments, most likely because of receptor binding of this protein. The cytoplasmic distribution of the dextran lasted even after the 24 hr incubation, whereas no such cytoplasmic distribution is seen without Ca^{2+} treatment. This cytoplasmic distribution of the dextran in

the Ca^{2+}-treated cells very strongly supports the contention that Ca^{2+} treatment induces endosomal escape of molecules such as PNA and dextran.

The calcium concentrations needed for optimal effect are much higher than physiological concentrations (micromolar range); therefore, the present findings are hardly relevant for in vivo delivery and bioavailability of cationic peptides and conjugates. However, they demonstrate that agents that trigger endosomal release should be of great interest. We also believe that our findings are generally applicable to most or all agents that are intrinsically cationic, such as lysine or arginine backbone-modified PNAs [24–27], cationic peptides [7, 10, 11, 13, 23], proteins [17], or polyamines.

Significance

The present study clearly shows that low millimolar concentrations of Ca^{2+} significantly enhance the nuclear antisense effects of PNA oligomers conjugated to oligoarginine or to Tat peptide. The detailed mechanism of the Ca^{2+} enhancement is not clear, but the data strongly indicate that both increased membrane association and, probably more importantly, increased endosomal release of the PNA are involved. In direct support of the latter mechanism, dextran (as a fluid-phase marker) is released from endosomes by Ca^{2+}. It is particularly noteworthy that the Tat conjugate is as active as the Arg_7 conjugate in the presence of Ca^{2+} despite the fact that it is much less active in the absence of Ca^{2+}. This finding would indicate that the mechanism(s) of cellular uptake of Tat and oligoarginine peptides differ in some aspect(s), which most likely include higher (spontaneous) endosomal escape of the oligoarginines. Although our results do only reflect PNA activity in the nucleus, the nuclear membrane would not be expected to be a major barrier for PNA-peptide conjugates; analogous experiments analyzing the cytoplasmatic effect of the PNAs as well as the effect of Ca^{2+} on this are underway. As we observe very little PNA in the nucleus (by confocal microscopy), the data also suggest that, despite being taken up by the cell, a major part of the PNA is trapped in a nonproductive compartment and that significant improvement in biological efficacy should be obtainable if more efficient enhancing compounds than Ca^{2+} can be discovered, further improving the potency of PNA. Clearly, these results are directly relevant for delivery of other cationic PNA derivatives, as well as for other (therapeutic) agents that rely on endosomal escape for bioavailability. It would be of particular interest if such compounds or regimes would be applicable in vivo.

Experimental Procedures

Synthesis of PNAs

The sequences and nomenclature of the PNAs are listed in Table 1. PNA synthesis was carried out as reported previously [19]. The PNAs were HPLC-purified and characterized by mass spectrometry. Cationic peptides were covalently linked to PNA at the N-terminal through an ethyleneglycol linker (eg1, 8-amino-2,6-dioxaoctanoic acid) or glycine via continuous synthesis. Fluorescein (Fl)-labeled PNA oligomers were prepared using a previously described "fluorescein-lysine" monomer [20]. The PNAs were lyophilized and stored at 4°C until use.

Cell Culture

HeLa pLuc705 cell line was purchased from GENE TOOLS (USA). The cells were cultured in RPMI-1640 medium (Sigma) supplemented with 10% fetal bovine serum (FBS), 1.5% glutamax (GIBCO), and streptomycin/penicillin (100 U/ml each) at 37°C in humidified air with 5% CO_2. For the transfection studies in 96-well plate format, cells were trypsinized and seeded (1.2×10^4 cells/well) 16 hr before transfection. For the 24-well plate, 7.2×10^4 cells/well were used.

PNA Transfection

HeLa pLuc705 cells, replated in 96-well plates 16 hr earlier, were treated with 100 μl/well of OPTI-MEM (GIBCO) containing the PNA at the desired concentration. For the Ca^{2+} or CQ supplementation studies, $CaCl_2$ or CQ was added to the OPTI-MEM at the desired concentration. After 4 hr incubation, the cells were supplemented with 100 μl/well of the growth medium (RPMI-1640 containing 10% FBS and 1.5% glutamax) and incubated further for 20 hr. For the transfection in 24-well plate format, 0.25 ml/well of OPTI-MEM and growth medium were used.

Luciferase Assay

At 24 hr after PNA treatment, the cells in the 96-well plate were subjected to luciferase activity measurements. Luciferase activity was measured with Fluoroskan Ascent FL (Labsystems) by using the Bright-Glo Luciferase assay system (Promega). Measurements were performed according to the manufacturers' instructions. Luminescent readings (with background subtracted) are presented as RLUs.

Cytotoxicity Test

At 24 hr after PNA treatment, the cells in the 96-well plate were subjected to the cell viability test. Cell viabilities were determined by using the CellTiter 96 Aqueous Non-Radioactive Cell Proliferation Assay (Promega) according to the manufacturer's instructions. The absorbance of treated cells was normalized to the absorbance of untreated cells (the value of the control was counted as 100%) and is presented as relative cellular viability.

Confocal Microscopy

Exponentially growing cells were plated in a 4-well Lab-Tek chambered coverglass (Nunc) the day before transfection. For the PNA transfection studies, cells were incubated with OPTI-MEM medium, including 1 μM of $(Arg)_7$-Fl-PNA and 20 μg/ml Alexa Fluor 633-conjugated human transferrin (80 kDa, Molecular Probes) with or without addition of 6 mM Ca^{2+}. After 15 min, the cells were washed and incubated further for 45 min in a fresh OPTI-MEM medium, and then analyzed using a MultiProbe 2001 Laser Scanning Confocal System equipped with an argon laser and a red laser diode (excitation and absorbance wavelengths, 488 nm and 638 nm, respectively; Radiance2000, BioRad) connected to a Nikon Eclipse TE200 microscope (oil immersion 60× 1.4 NA objective; Nikon, Tokyo, Japan). The Lasersharp 2000 software package (BioRad) was used for image acquisition and processing.

For the dextran uptake studies, cells were incubated with OPTI-MEM, including 2 mg/ml of FITC-labeled dextran (10 kDa, Sigma) and 20 μg/ml of Alexa Fluor 633-conjugated human transferrin in the absence or presence of 6 mM Ca^{2+} for 4 hr. Cells were then incubated further in fresh growth medium for 1 or 24 hr and subjected to confocal microscopy analysis as described above.

Flow Cytometry

HeLa pLuc705 cells were plated in 24-wells plates the day before the experiment. Immediately prior to transfection, cells were washed once with PBS and treated with 1 μM of $(Arg)_7$-Fl-PNA in OPTI-MEM in the presence or absence of 6 mM Ca^{2+}. For the flow cytometry analysis, cells were collected by scraping (Trypsin–) or by trypsination (Trypsin+). For the scraping method, cells from one well were collected by scraping and subjected to the analysis in 400 μl PBS. For trypsination, cells were washed with PBS three

times and trypsinized for 6 min at 37°C followed by the addition of 300 μl growth medium. Cells were then washed once and subjected to the analysis in 400 μl PBS. Cells (2000 events) were analyzed using a BD FACSCalibur cytometer, and the mean fluorescence signal was sampled by CellQuest software. The fluorescence index was calculated by dividing the mean fluorescence of the PNA-treated sample by the mean fluorescence of a control sample (without PNA treatment).

RT-PCR

Exponentially growing cells were cultured in 24-well plates the day before treatment. Treatment with PNA was performed as described above. After 24 hr, total RNA was extracted from the cells by using RNeasy Mini kit (Qiagen) and subjected to RT-PCR. RT-PCR was performed using OneStep RT-PCR kit (Qiagen). A total of 3 ng RNA was used for each RT-PCR reaction (20 μl). Primers for the RT-PCR were as follows: forward primer, 5′-TTGATATGTGGATTTCGAGTC GTC-3′; reverse primer, 5′-TGTCAAT-CAGAGTGCTTTTGGCG-3′. The RT-PCR program was as follows: ([55°C, 35 min] × 1 cycle; [95°C, 15 min] × 1 cycle; [94°C, 0.5 min; 55°C, 0.5 min; 72°C, 0.5 min] × 30 cycles). RT-PCR products were analyzed on 2% agarose gel with 1× TBE buffer and visualized by ethidium bromide staining. Gel images were captured by ImageMaster (Pharmacia Biotech) and analyzed by UN-SCAN-IT software (Silk Scientific Corporation).

Acknowledgments

This study was supported by the Danish Cancer Society, The Lundbeck Foundation (senior research fellowship to T.S.), and the Danish Medical Research Council. The authors acknowledge Darya Kiryushko for help with the confocal laser microscope, and Dr. Raino Hansen for fruitful discussions in the initial phase of the project.

Received: April 12, 2005
Revised: June 9, 2005
Accepted: June 9, 2005
Published: August 26, 2005

References

1. Nielsen, P.E., Egholm, M., Berg, R.H., and Buchardt, O. (1991). Sequence-selective recognition of DNA by strand displacement with a thymine-substituted polyamide. Science *254*, 1497–1500.
2. Juliano, R.L., Alahari, S., Yoo, H., Kole, R., and Cho, M. (1999). Antisense pharmacodynamics: critical issues in the transport and delivery of antisense oligonucleotides. Pharm. Res. *16*, 494–502.
3. Doyle, D.F., Braasch, D.A., Simmons, C.G., Janowski, B.A., and Corey, D.R. (2001). Inhibition of gene expression inside cells by peptide nucleic acids: effect of mRNA target sequence, mismatched bases, and PNA length. Biochemistry *40*, 53–64.
4. Bendifallah, N., Kristensen, E., Dahl, O., Koppelhus, U., and Nielsen, P.E. (2003). Synthesis and properties of ester-linked peptide nucleic acid prodrug conjugates. Bioconjug. Chem. *14*, 588–592.
5. Mologni, L., Marchesi, E., Nielsen, P.E., and Gambacorti-Passerini, C. (2001). Inhibition of promyelocytic leukemia (PML)/retinoic acid receptor-alpha and PML expression in acute promyelocytic leukemia cells by anti-PML peptide nucleic acid. Cancer Res. *61*, 5468–5473.
6. Muratovska, A., Lightowlers, R.N., Taylor, R.W., Turnbull, D.M., Smith, R.A., Wilce, J.A., Martin, S.W., and Murphy, M.P. (2001). Targeting peptide nucleic acid (PNA) oligomers to mitochondria within cells by conjugation to lipophilic cations: implications for mitochondrial DNA replication, expression and disease. Nucleic Acids Res. *29*, 1852–1863.
7. Richard, J.P., Melikov, K., Vives, E., Ramos, C., Verbeure, B., Gait, M.J., Chernomordik, L.V., and Lebleu, B. (2003). Cell-penetrating peptides: a reevaluation of the mechanism of cellular uptake. J. Biol. Chem. *278*, 585–590.
8. Thoren, P.E., Persson, D., Isakson, P., Goksor, M., Onfelt, A., and Norden, B. (2003). Uptake of analogs of penetratin, Tat(48–60) and oligoarginine in live cells. Biochem. Biophys. Res. Commun. *307*, 100–107.
9. Filipovska, A., Eccles, M.R., Smith, R.A., and Murphy, M.P. (2004). Delivery of antisense peptide nucleic acids (PNAs) to the cytosol by disulphide conjugation to a lipophilic cation. FEBS Lett. *556*, 180–186.
10. Koppelhus, U., Awasthi, S.K., Zachar, V., Holst, H.U., Ebbesen, P., and Nielsen, P.E. (2002). Cell-dependent differential cellular uptake of PNA, peptides, and PNA-peptide conjugates. Antisense Nucleic Acid Drug Dev. *12*, 51–63.
11. Aldrian-Herrada, G., Desarmenien, M.G., Orcel, H., Boissin-Agasse, L., Mery, J., Brugidou, J., and Rabie, A. (1998). A peptide nucleic acid (PNA) is more rapidly internalized in cultured neurons when coupled to a retro-inverso delivery peptide: the antisense activity depresses the target mRNA and protein in magnocellular oxytocin neurons. Nucleic Acids Res. *26*, 4910–4916.
12. Cutrona, G., Carpaneto, E.M., Ponzanelli, A., Ulivi, M., Millo, E., Scarfi, S., Roncella, S., Benatti, U., Boffa, L.C., and Ferrarini, M. (2003). Inhibition of the translocated c-myc in Burkitt's lymphoma by a PNA complementary to the E mu enhancer. Cancer Res. *63*, 6144–6148.
13. Moulton, H.M., Nelson, M.H., Hatlevig, S.A., Reddy, M.T., and Iversen, P.L. (2004). Cellular uptake of antisense morpholino oligomers conjugated to arginine-rich peptides. Bioconjug. Chem. *15*, 290–299.
14. Kang, S.H., Cho, M.J., and Kole, R. (1998). Up-regulation of luciferase gene expression with antisense oligonucleotides: implications and applications in functional assay development. Biochemistry *37*, 6235–6239.
15. Fuchs, S.M., and Raines, R.T. (2004). Pathway for polyarginine entry into mammalian cells. Biochemistry *43*, 2438–2444.
16. Zaitsev, S., Buchwalow, I., Haberland, A., Tkachuk, S., Zaitseva, I., Haller, H., and Bottger, M. (2002). Histone H1-mediated transfection: role of calcium in the cellular uptake and intracellular fate of H1-DNA complexes. Acta Histochem. *104*, 85–92.
17. Haberland, A., Knaus, T., Zaitsev, S.V., Stahn, R., Mistry, A.R., Coutelle, C., Haller, H., and Bottger, M. (1999). Calcium ions as efficient cofactor of polycation-mediated gene transfer. Biochim. Biophys. Acta *1445*, 21–30.
18. Bottger, M., Zaitsev, S.V., Otto, A., Haberland, A., and Vorob'ev, V.I. (1998). Acid nuclear extracts as mediators of gene transfer and expression. Biochim. Biophys. Acta *1395*, 78–87.
19. Christensen, L., Fitzpatrick, R., Gildea, B., Petersen, K.H., Hansen, H.F., Koch, T., Egholm, M., Buchardt, O., Nielsen, P.E., Coull, J., et al. (1995). Solid-phase synthesis of peptide nucleic acids. J. Pept. Sci. *1*, 175–183.
20. Lohse, J., Nielsen, P.E., Harrit, N., and Dahl, O. (1997). Fluorescein-conjugated lysine monomers for solid phase synthesis of fluorescent peptides and PNA oligomers. Bioconjug. Chem. *8*, 503–509.
21. Mitchell, D.J., Kim, D.T., Steinman, L., Fathman, C.G., and Rothbard, J.B. (2000). Polyarginine enters cells more efficiently than other polycationic homopolymers. J. Pept. Res. *56*, 318–325.
22. Ciftci, K., and Levy, R.J. (2001). Enhanced plasmid DNA transfection with lysosomotropic agents in cultured fibroblasts. Int. J. Pharm. *218*, 81–92.
23. Kaihatsu, K., Huffman, K.E., and Corey, D.R. (2004). Intracellular uptake and inhibition of gene expression by PNAs and PNA-peptide conjugates. Biochemistry *43*, 14340–14347.
24. Haaima, G., Lohse, A., Buchardt, O., and Nielsen, P.E. (1996). Peptide nucleic acids (PNAs) containing thymine monomers derived from chiral amino acids: hybridization and solubility properties of D-lysine PNA. Angew. Chem. *35*, 1939–1941.
25. Püschl, A., Sforza, S., Haaima, G., Dahl, O., and Nielsen, P.E. (1998). Peptide nucleic acids (PNAs) with a functional backbone. Tetrahedron Lett. *39*, 4707–4710.
26. Ljungstrøm, T., Knudsen, H., and Nielsen, P.E. (1999). Cellular uptake of adamantyl conjugated peptide nucleic acids. Bioconjug. Chem. *10*, 965–972.
27. Zhou, P., Wang, M., Du, L., Fisher, G.W., Waggone, R.A., and Ly, D.H. (2003). Novel binding and efficient cellular uptake of guanidine-based peptide nucleic acids (GPNA). J. Am. Chem. Soc. *125*, 6878–6879.